

Evaluating Light Pollution: An IES Model for Intervention Strategies

Ruixi Su¹, Yi Chen² & Zibin Huang³

¹ School of Artificial Intelligence, Sun Yat-sen University, Zhuhai, China

² College of Physics and Optoelectronic Engineering, Shenzhen University, Shenzhen, China

³ Guangzhou Dublin International College of Life Sciences and Technology, South China Agricultural University, Guangzhou, China

Correspondence: Zibin Huang, Guangzhou Dublin International College of Life Sciences and Technology, South China Agricultural University, Guangzhou, China. Tel: 159-9232-4108. E-mail: 2033828815@qq.com

Received: May 28, 2023

Accepted: August 7, 2023

Online Published: August 10, 2023

doi:10.5539/ep.v13n1p1

URL: <https://doi.org/10.5539/ep.v13n1p1>

Abstract

There is an increasing urgency to address how the light pollution risk level can be accurately and comprehensively measured and evaluated. Based on current research and data, this paper proposes a model concerning light pollution risk levels applicable to various regions. Optimized intervention strategies are then provided to reduce the effect of light pollution. For one thing, this paper establishes an *Illumination-Environment-Society Evaluation* (IES) model to evaluate a region's light pollution risk level. Primary indicators of the model involve three dimensions, each quantified by 2 to 5 secondary indicators, with sufficient data analysis conducted, including data rasterization of satellite remote sensing images, *K*-means clustering analysis, *Principal Component Analysis* (PCA), *Entropy Weight Method* (EWM), *Technique for Order Preference by Similarity to Ideal Solution* (TOPSIS), *Analytic Hierarchy Process* (AHP), and other assistant algorithms. In this regard, the present study obtains and grades some regions' light pollution risk levels. For another, this paper determines three possible intervention strategies for light pollution based on the IES model after interpreting the results. Non-linear programming methods are also employed to optimize these three strategies. The present study aims to exploit a new avenue for relevant environmental research, providing references for light pollution measurement and intervention.

Keywords: light pollution risk level, IES Model, intervention strategies, AHP, EWM-TOPSIS

1. Introduction

Light pollution is a common social problem. Nightscape lighting plays a critical role in shaping the night image and improving the life service environment in modern times. At the same time, the boost of urbanization, infrastructure upgrading, semiconductor lighting, and digital technology innovation and application is triggered by the surge of artificial lighting design. Reality comes, however, that not all lighting achieves this effect. The rapid global increase in artificial light at night has been proposed as a new threat to terrestrial ecosystems (Falchi *et al.*, 2016; Knop *et al.*, 2017). When lighting harms people, plants, animals, and the environment, it develops into light pollution, which is not conducive to the sustainable development of society.

The negative impact of light pollution is becoming increasingly conspicuous nowadays. Light pollution is considered to be the phenomenon of excessive optical radiation causing adverse effects on human living and the production environment. Nevertheless, the impact of light pollution on humanity is growing prominent, and it may grow into ecological pollution affecting both the human and natural environment. Adverse effects of inappropriate lighting on health vary vastly, including instantaneous and long-term cumulative effects and perceived and potential impacts. Hence, research on the nature and control of light pollution has evolved into an academic issue concerning the global environment (Shing *et al.*, 2012; Kyba *et al.*, 2015; Ścieżor, 2021).

This paper aims to establish an *Illumination-Environment-Society Evaluation* (IES) model for light pollution evaluation. This model first measures and mitigates the effects of light pollution in various regions while considering both human and non-human factors. Moreover, it provides a broadly applicable metric to assess a region's light pollution risk level and apply it to four distinct locations. After analyzing the results, three potential light pollution intervention strategies are proposed, grounding the IES model, including specific steps to be adopted and their potential impacts on the effects of light pollution. Eventually, one appropriate and representative intervention strategy for two locations is selected based on the metric, and relevant effects on the location's risk

level are also discussed before moving to the conclusion.

2. Literature Review

2.1 An Overview of Light Pollution

A series of studies have been carried out on the further severity of light pollution. As an epochal product of industrialization and urbanization, light pollution can be defined as artificial light contributing to the night sky (Cavazzani *et al.*, 2020; Simons *et al.*, 2020). The awareness of light pollution traces back to astronomical studies in the 1930s (Luginbuhl *et al.*, 2009) when city lights were too bright and significantly impacted astronomical observations. Light pollution in the night sky makes observations of astronomical objects very difficult when cumulative light above large cities degrades the quality of observations, especially for the observatories (Grunkowski *et al.*, 2018). At that time, people's limited understanding of light pollution led them to focus on astronomical light pollution that made the starry sky disappear. However, in recent years, many cities have started lighting projects with economic development and urbanization promotion. In this case, light pollution also becomes an ecological problem besides its negative effect on astronomy (Navara & Nelson, 2007). The number of functional areas, such as leisure areas, to enhance the city's night landscape and commercial concentration areas, mainly to enhance the business environment, has increased year by year, which to some extent leads to the city becoming brighter and brighter at night (Falchif *et al.*, 2016). This problem worsens as artificially lit outdoor areas are growing by 2.2% per year, and continuously lit areas are brightening by 2.2% each year, likely due to the rapid growth in population and urbanization (Kyba *et al.*, 2017). The problem of light pollution has seriously damaged the natural environment and become an ecological pollution affecting human beings and the natural environment, which has also become one of the most rapidly increasing problems of changing the natural environment (Gallaway *et al.*, 2010). Relevant research (e.g., Prakash *et al.*, 2017; Ouyang *et al.*, 2017; Wakefield *et al.*, 2018; Vandersteen *et al.*, 2020; Pauwels *et al.*, 2021; Brayley *et al.*, 2022) has been carried out to show how light pollution affects the population and functioning of various species of insects, birds, and bats. Thus, light pollution gradually attracts attention and has become a severe global environmental issue (Navara & Nelson, 2007; Falchi *et al.*, 2011; Alamús *et al.*, 2017; Hussein *et al.*, 2020).

Compared with other pollutions, light pollution is a relatively new concept. From the internationally accepted standards, light pollution is not only about the disappearance of the starry sky due to astronomical light pollution. What is more serious is the impact of its wide range, non-cumulative, transient characteristics, human health, and ecological environment. Types of light pollution include glare (excessive brightness that causes visual discomfort), skyglow (lighting up the night sky), light trespass (lights falling in unintended or unwanted places), and clutter (bright, confusing, and excessive light source components) (cf. Falchi *et al.*, 2011). To a certain degree, light pollution is the inappropriate or excessive use of artificial light, resulting in serious environmental consequences for humans, wildlife, and the climate.

2.2 Effects of Light Pollution

Light pollution harms humans, economy, ecology, and biodiversity in many aspects. For the human body, the glass curtain wall reflects and refracts the daytime sunlight and night lighting, which causes significant irritation to human eyes. Studies (e.g., Salthammer, 2011; Frontczak & Wargocki, 2011) have shown that urban populations spend more than 15-16 hours per capita per day indoors.

The harm of light pollution on the ecological environment mainly includes the effect on the natural life pattern of animals, the disruption of the biological clock rhythm in plants, and ecological imbalance^{1,2,3}. *Artificial light at night* (ALAN), which is rapidly spreading globally at an estimated rate of 6% per year (Hölker *et al.*, 2010), has been shown to affect the physiology and behavior of various organisms (Gaston *et al.*, 2013). ALAN changes or even destroys the natural light cycle, range, and intensity, which strongly interferes with the reproduction and migration of animals and accelerates or postpones the growth cycle of plants. This affects biodiversity to varying degrees and disrupts the entire ecosystem cycle chain (Van *et al.*, 2017). Hölker *et al.* (2015) conducted field and laboratory experiments using sediments from agricultural drainage systems and found that ALAN affects microbial diversity and community respiration in freshwater sediments. The above studies show that ALAN can profoundly affect species communities and population dynamics.

Many existing studies attempt to evaluate the impact of light pollution on the economy. Gallaway *et al.* (2010) first consider the economic factors contributing to global light pollution. It is found that both population and Gross

¹ <https://www.health.harvard.edu/staying-healthy/blue-light-has-a-dark-side>.

² <https://www.darksky.org/light-pollution/wildlife/>.

³ <https://islandpress.org/books/ecological-consequences-artificial-night-lighting>.

Domestic Product (GDP) are significant explanatory variables for light pollution, similar to other types of pollution. Related studies assess the relationship between economic development and light pollution (e.g., Jack *et al.*, 2018). Examples given by Elvidge *et al.* (1999), Hara *et al.* (2010), Shi *et al.* (2014), and Lin & Shi (2020) correlate human activities, such as electric consumption, to the energy escaping to space. A solid and obvious correlation exists between power consumption and artificial light observed in space, as noted by de Miguel *et al.* (2014). According to *the International Dark Sky Association*, at least 30% of outdoor lighting in the United States is wasted yearly, resulting in about \$3.3 billion in energy loss and 21 million tons of carbon dioxide.⁴

2.3 Measures and Intervention of Light Pollution

The measurement of the impact of light pollution on humans was a critical issue (Fryc *et al.*, 2022). In recent years, the biosafety of light radiation has received significant attention, and *the International Commission on Illumination* (CIE), *the International Electrotechnical Commission* (IEC), *Europe* (EN), and *the American National Standards Organization* (ANSI) have developed biosafety standards for light radiation. Numerous measurement techniques are utilized for the monitoring and analysis of light pollution, including *the Sky Quality Meter* (SQM) photometers (Zamorano *et al.*, 2016; Puschnig *et al.*, 2019), *Satellite Base Defense Meteorological Satellite Program-Operational Line-Scan System* (DMSP/OLS), *International Space Station* (ISS) night time light measurements (Kuffer *et al.*, 2018), and *the Visible Infrared Imaging Radiometer Suite* (VIIRS) (Levin *et al.*, 2019). These techniques provide invaluable insights into the impact of light pollution on various environmental and societal aspects.

Besides, many studies relate to measurement techniques and light pollution monitoring. Appropriate hardware solutions are created and sometimes combined into entire measurement networks that enable the analysis of the surface brightness of the night sky (Bertolo *et al.*, 2019; Karpińska & Kunz, 2022). The influence of weather conditions on the obtained results is analyzed (Ścieżor, 2020). There is also great interest in using crewless aerial vehicles to quickly inspect light pollution in a given area (Tabaka, 2020; Bouroussis & Topalis, 2020). Moreover, the interest is also given in analyzing luminance distribution on a night sky, building surfaces, or lighting equipment using luminance cameras (e.g., Hänel *et al.*, 2018; Galatanu *et al.*, 2019; Czyżewski *et al.*, 2023; Słomiński & Krupiński *et al.*, 2018). Existing studies evaluate the light pollution risk level in illuminance factor, and this study innovatively considers environmental and social factors on the light pollution level.

Aware of the urgency of addressing light pollution, international organizations have been working to reduce light pollution, such as *the International Dark Skies Association* (IDA), which focuses on public science and certifies other areas that work towards effectively reducing light emissions. As of December 2018, IDA listed 13 dark sky-protected areas on its website. CIE has extensively researched interference light control and issued *the Guidelines for Limiting the Impact of Interference Light from Outdoor Lighting Facilities* (CIE 150, now referred to as *The Guidelines*). *The Guidelines* are an essential basis and reference for developing relevant standards in interference light control in China (Pollard, 2001), and its revision in 2017 proposed to set the ambient brightness zoning into five categories (see Table 1).

Table 1. Environment lighting zones

Ambient Brightness Zoning	Ambient Brightness	Zone
E0	Total Darkness	<i>United Nations Educational, Scientific and Cultural Organization</i> (UNESCO) Starlight Reserve, IDA Dark Sky Park, Important Optical Astronomy Observatory
E1	Darkness	Uninhabited rural areas
E2	Low brightness area	Sparsely populated rural areas
E3	Medium brightness area	Inhabited rural and urban settlements
E4	High brightness area	Town centers and other commercial areas

The Guidelines analyze the problem of light interference from four aspects: residential areas, traffic logistics, landscaping, and astronomical observation. According to different degrees of brightness, the environmental

⁴ <https://www.darksky.org/light-pollution/energy-waste/>.

brightness is divided into five intervals (E0~E4), giving a variety of outdoor lighting conditions, different environmental intervals of photometric parameters limits, including the vertical illumination of the house (light intrusion) limits, the luminosity limits of lamps in the field of view, the brightness of the light curtain in road lighting and threshold increment limits, the control of the sky glow of the lamps on the luminous flux ratio limits, intense light to light the building facade and the luminance limit value of signage signs.

Many countries have formulated relevant laws, regulations, and technical specifications according to national conditions. However, no unified light pollution prevention and control standard applies to each country internationally because of each country's architectural characteristics and customs. This paper innovatively combines mathematical models with light pollution prevention and control standard indicators, aiming to use mathematical calculations to comprehensively calculate the parameters that can comprehensively represent the prevention and control standards and provide a new direction for light pollution prevention and control research.

3. Methodology

3.1 Research Design

The present study is designed as follows (see Figure 1 and the following explanations).

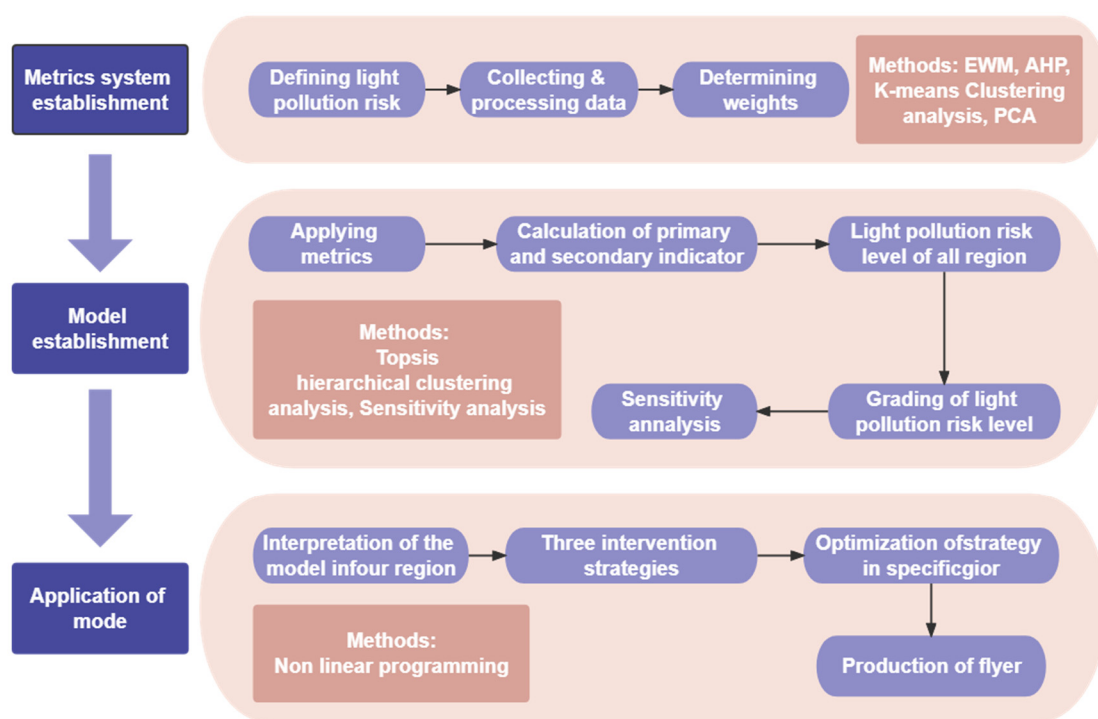


Figure 1. Research design

a) **Build a metrics system.** Firstly, light pollution risk is defined by relevant indicators. The second step is to search and process relevant data in various databases. Finally, these processed data are used to determine the metric weights. EWM, AHP, *K*-means clustering analysis, and PCA methods are used to promote the foundation of this metric system.

b) **Establish a model.** First, the processed metric helps define light pollution risk levels in different regions. Moreover, the calculation of primary and secondary indicators is processed to attain light pollution risk levels of different regions. Next, light pollution risk levels are graded to classify different regions. Ultimately, the model is evaluated by sensitivity analysis to prove its applicability. TOPSIS and hierarchical clustering analysis are applied in this section.

c) **Application of model.** The interpretation of the model in four regions is illustrated. Furthermore, three intervention strategies are determined with the optimization for the specific condition. Non-linear programming is used in this section.

3.2 Notions, Assumptions, and Justifications

The critical mathematical notations used in this paper are listed in Table 2.

Table 2. Notations used in this paper

Symbol	Description	Unit
I	Illuminance Level	digital number
L	Luminaire Density Distribution	/
Q	Replacement Quantity	thousand luminaire
R	Substitution Index	percentage
D	Average Duration of Light	hour
x	Turn-off Time of Luminaires	hour
B	Biodiversity Indicator	population/km ²
P	Data on Population Density	population/km ²

There are three assumptions for the present study. First, light pollution risk levels in given areas are assumed to be stable over a short period. From a relatively synchronic perspective, barring severe, unpredictable natural disasters or wars, changes in light pollution risk levels in the same area within a short time can be ignored. In addition, relevant intervention strategies are assumed to be implemented. In this regard, the effectiveness of these strategies can be evaluated, though there may be some unexpected factors that influence the employment of these strategies. Last but not least, the data are assumed to reflect the characteristics of those indicators. The data used in the model were mainly collected from influential statistical websites and satellite data, which can more or less signal the reliability and credibility of the metric.

4. An IES Model for Light Pollution Risk Level

This section establishes the IES Model by considering overall metrics to assess light pollution risk levels. This metric system is applied to four categories of locations with the interpretation of their results. After referring to the pre-processed data of NPP-VIIRS, three primary indicators are attained by comparing relevant dimensions in different regions: illumination, environment, and society. In this paper, light pollution risk levels measure and evaluate light output and environmental and societal factors on artificial light generation in a given area.

4.1 The Establishment of the IES Model

Figure 2 depicts an essential representation of the model. It comprises three primary and eight secondary indicators to form a complete metrics system. More details are provided in this section.



Figure 2. Primary and secondary indicators in the IES model

4.1.1 Illumination Output Indicators

The amount of illumination output directly impacts the light pollution level in a specific area. As a result, measuring the amount of light pollution in a region must determine how much light is produced there. In this model, the illuminance level, luminaire density distribution, and average light duration are secondary indicators for calculating the light emitted from a given region.

It should be noted that surface reflectance determines the diffusion intensity of natural light on the surface of an object and is an important indicator that affects the degree of light pollution. However, the results of surface reflection are still covered in illumination level and luminaire density distribution (measured by DMSP/OLS light images).

a) Illuminance level

The illuminance level can be assessed through night illuminance, as relevant data can be collected precisely. The NPP-VIIRS night light survey data, pre-processing the data (such as rasterization), using ENVI and ArcGIS for data analysis, and obtaining the *digital number* (DN) value are all done in this manner. DN refers to the remote sensing image's pixel brightness value or the sensor's digital quantization output value, similar to an image's gray value. It frequently refers to pixel values that must be calibrated to valuable units. As a result, it has no unit. It is an integral value that depends on factors such as the sensor's radiation resolution, the emissivity of nearby objects, and the atmospheric transmittance and scattering rate, among others. The reflectance of the outer surface of the atmosphere can be used to convert radiometric calibration based on the original DN values that are recorded. Meanwhile, DN values of each region need to be processed with Z-score standardization before application.

$$\sigma = \sqrt{\frac{1}{N} \sum_{i=1}^N (X_i - \mu)^2}$$

Among them, N is the sample value of the DN value, and μ is the sample's mean.

$$\mu = \frac{\sum_{i=1}^N X_i}{N}$$

Finally, the transformation formula is:

$$Z_i = \frac{X_i - \mu}{\sigma}$$

In the formula, Z_i is the illuminance level indicator of each area after standardization.

b) Luminaire density distribution

Luminaire density distribution refers to the intensity of luminaire brightness per unit area. DMSP/OLS light images are used for K-means clustering analysis and data visualization for the density distribution of luminaires. Finally, the contour coefficient and other indicators are used to evaluate the clustering results to determine the best clustering results and the density distribution indicator of luminaires. Via cluster analysis, the distribution indicator of luminaire density in different regions of China is attained (see Figure 3).

c) The average duration of light

The average duration of light is the duration of artificial light exposure per unit of time in a given area. This indicator must be normalized with a Z-score (calculated using the same formula as the illuminance level) for the average light density in a particular area.

4.1.2 Environment Indicators

Previous studies (e.g., Chen & Peng, 2013; Ding *et al.*, 2014; Gao *et al.*, 2019; Hao *et al.*, 2022) have shown that environmental indicators are thought to influence light pollution risk levels in specific areas closely. Thus, including environmental factors as indicators to assess the light pollution risk level is valid. Environmental indicators include geography, biodiversity, and climate.

a) Geography

Geographical indicators refer to factors such as land use and air quality levels. Relevant literature (e.g., Nian *et al.*, 2005; Zhang *et al.*, 2007) reveals a robust logical correlation between land use, air quality, and light pollution risk in a region. Based on year-round sunshine and air quality levels, the calculation is presented as follows.

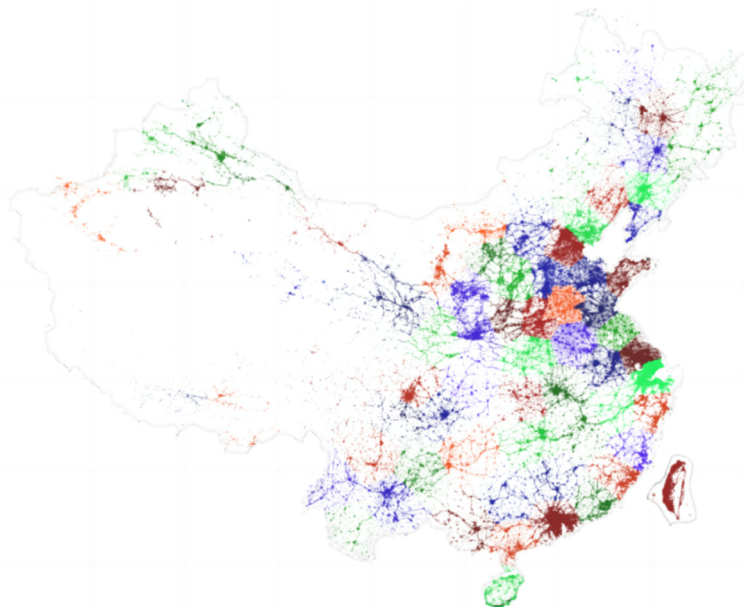


Figure 3. Distribution index of luminaire density in different regions of China

First, data on air quality level and land use are normalized, respectively:

$$Y_i = \frac{X_i - Min}{Max - Min}$$

Among them, Min is the minimum of two types of the initial data set, while Max is the maximum. Then, after conducting a *chi-square* test on air quality level and land use, this paper discovers that the correlation between the two data types is very weak. Therefore, this paper chooses to average the two groups of data based on the region and obtain the geographical indicators:

$$Z_i = \frac{Y_{i1} + Y_{i2}}{2}$$

In the formula, Y_{i1} represents the air quality level in region i , while Y_{i2} represents the utilization level of region i . Finally, the value should be normalized and Z-score standardized (the calculation formula is the same as the illuminance level).

b) Biodiversity

Biodiversity refers to indicators such as the area's green coverage. Even though the detrimental effects of artificial light at night on different organisms, including humans, have been subject to research and communication more intensively during the last decades (Longcore & Rich, 2004; Hölker *et al.*, 2010). Whereas temperature, food, exercise, and even reward can all serve as "zeitgebers," or timekeepers, the light remains the strongest, most potent entraining zeitgeber for the circadian system (Challet & Pévet, 2003). Artificial light at night has been shown to affect the physiology and behavior of various organisms (Gaston *et al.*, 2013). Regional biological diversity considerably affects the light pollution risk level as an influential element. In nature reserves, for instance, a high light pollution level will significantly impact creatures' survival. For example, light-induced bird-building collisions have been known to science for more than 150 years (e.g., Korner *et al.*, 2022). Knop *et al.* (2017) focused on the effect of artificial light at night on plant pollination, and they found that artificial light at night disrupts nocturnal pollination networks and negatively affects the reproductive on of plants.

Nevertheless, relevant research discloses that birds are substantially more susceptible to light pollution than other animal species. Consequently, the model uses the regional bird distribution density and species amount as a metric for animal diversity. Research (e.g., Dong, 2008; Zhang *et al.*, 2019) shows a solid logical correlation between green coverage and light pollution risk levels in specific areas. Therefore, vegetation coverage is considered an indicator of plant diversity.

The calculation method is as follows. Firstly, the data is pre-processed. Similarly, normalization and Z-score standardization are carried out for this indicator. Secondly, this indicator has two dimensions; thus, this research

considers data dimensionality reduction through PCA. Finally, a comprehensive indicator of biodiversity is gained.

c) Climate

Climate indicators refer to relative humidity, precipitation, and average temperature. It is found that relative humidity, precipitation, and average temperature significantly influence the light pollution risk level, among which relative humidity and precipitation are highly correlated. Only the relative humidity and average temperature are considered to reduce the overlap of indicators, which significantly impact light pollution. The calculation method is as follows.

It is worth noting that climate indicators include relative humidity and average temperature. Considering that seasonal changes influence the degree of light pollution, the data is an annualized average.

First, the two average temperature datasets are normalized and standardized via Z-score. As for the humidity indicator, due to the negative correlation between humidity and light pollution compared with other indicators, this paper carries out normalization and Z-score standardization after the positive normalization of this indicator. The positive method is as follows:

$$H_i = Max - H_{0i}$$

Among them, H_{0i} is the annual relative humidity of region i , and Max is the maximum annual relative humidity. Then, this paper takes its mean value as the climate indicator value.

$$X_i = H_i + T_i$$

For region i , X_i is the climate indicator value; H_i and T_i are the pre-processed relative humidity data and average temperature, respectively.

4.1.3 Social Indicators

Social indicators include population density, GDP, optical output, and environmental indicators. It is discovered that GDP and light pollution risk levels are strongly correlated, and population density also significantly impacts light pollution risk levels.

a) Population density

Population density is the number of people per unit of land area. Population always increases arithmetically, and population density can be shown to correlate with other demographic parameters, especially human activities affecting the environment (Elvidge *et al.*, 1999; Hara *et al.*, 2010; Shi *et al.*, 2014; Falchi *et al.*, 2016). Research (e.g., Su, 2011) shows that population density is usually positively correlated with the light pollution indicator because areas with high population density have higher light source utilization intensity, which has a higher impact on light absorption pollution. This paper also performs normalization and Z-score standardization processing for the population density indicator.

b) Gross Domestic Product (GDP)

GDP is the final result of all the resident units' production activities of a country (or region) in a certain period. Existing studies (e.g., Zhao & Xiang, 2003; Liu, 2007; Gao *et al.*, 2019) have shown a close relationship between GDP and the light pollution risk indicator. Normalization and Z-score standardization processing are supposed to be conducted for the population density indicator.

4.2 Determining Weights

The data used to evaluate the indicators comes from several databases, especially *the 2021 China Statistical Yearbook*. This paper focuses on data from different regions of China and calculates these indicators for every significant province and region in China.

Based on pre-processing of the above data (Z-score standardization and normalization) and related literature, EWM is first used to calculate the weight of each secondary indicator data. Then, the calculated weight is combined with the TOPSIS to calculate the score of each primary indicator. Finally, AHP is used to calculate the weight of the primary indicator.

4.2.1 Determining the Weight of Secondary Indicators by EWM

EWM is used to determine the weights of secondary indicators. First, the proportion of region i under the j -th indicator is calculated, and is taken as the probability for calculating relative entropy. Z_{ij} represents the data of the j -th indicator and the i -th sample point.

$$P_{ij} = \frac{Z_{ij}}{\sum_{i=1}^n Z_{ij}}$$

Among them, n is the total number of regions, and P_{ij} is the relative entropy of region i under the j -th indicator. Secondly, the information entropy of each indicator is calculated to obtain the information utility value. Finally, the information utility value is normalized to obtain the entropy weight of each indicator. For the j -th indicator, the calculation formula is as follows:

$$e_j = -\frac{1}{\ln n} \sum_{i=1}^n P_{ij} \ln(P_{ij})$$

Then, the coefficient of variation is calculated:

$$d_j = 1 - e_j$$

Ultimately, the information utility value is normalized and then calculated:

$$\omega_j = \frac{d_j}{\sum_{j=1}^m d_j}$$

4.2.2 Using TOPSIS with Obtained Weights for Primary Indicator Scores

After utilizing the above positive and standardized data, the following indicator matrix can be obtained:

$$Z = \begin{bmatrix} Z_{11} & \cdots & Z_{1m} \\ \vdots & \ddots & \vdots \\ Z_{n1} & \cdots & Z_{nm} \end{bmatrix}$$

Among them, n is the number of evaluation samples, while m is the value of indicators. Moreover, this research defines the following concepts further:

$$Z^+ = (Z_1^+, Z_2^+, \dots, Z_m^+)$$

$$Z^- = (Z_1^-, Z_2^-, \dots, Z_m^-)$$

$$Z_i^+ = \max\{Z_{1i}, Z_{2i}, \dots, Z_{ni}\}$$

$$Z_i^- = \min\{Z_{1i}, Z_{2i}, \dots, Z_{ni}\}$$

In the formula, Z^+ and Z^- are the maximal and minimum values of the TOPSIS indicator matrix, respectively. Then, the following calculations are conducted:

$$D_i^+ = \sqrt{\sum_{j=1}^m \omega_j (Z_j^+ - Z_{ij})^2}$$

$$D_i^- = \sqrt{\sum_{j=1}^m \omega_j (Z_j^- - Z_{ij})^2}$$

D_i^+ and D_i^- in the formula indicate the distance between the maximal and minimal values of the i -th evaluated objective and its indicator. Next, this research calculates the scores of the primary indicator are calculated:

$$S_i = \frac{D_i^-}{D_i^+ + D_i^-}$$

4.2.3 Using AHP for the Weights of Three Primary Indicators

AHP is utilized to confirm the weights of three primary weights. First, the pair comparison matrix is gained according to the relevant theories and literature. After that, the weight coefficient is calculated based on the following formula:

$$\beta_i' = \sqrt[n]{a_{i1} a_{i2} \cdots a_{in}}$$

Then, the weighted values are normalized:

$$\beta_i = \frac{\beta'_i}{\sum_{i=1}^n \beta'_i}$$

Finally, a consistency check is performed. The results show that the model is acceptable.

4.2.4 Calculating Comprehensive Weights and Scores

The IES model can measure a specific area’s light pollution risk indicator. The corresponding weights of primary and secondary indicators are obtained, as shown in Table 3.

Table 3. Weights of primary and secondary indicators

Primary Indicators	Weights	Secondary Indicators	Weights
Illumination Output Metrics	0.5576	Illuminance Level	0.5327
		Luminaire Density Distribution	0.3417
		Average Duration of Light	0.1256
Environment Metrics	0.2692	Geography	0.0736
		Biodiversity	0.8003
		Climate	0.1261
Social Metrics	0.1733	Population Density	0.5393
		GDP	0.4607

For the calculation of the comprehensive score, the method is as follows:

$$E_i = \beta_i S_i$$

$$E = \sum_{i=1}^n E_i$$

In the formula, E_i is the indicator calculated by the primary indicator, and E is the light pollution risk indicator calculated by the region.

With significant provinces and cities in China as examples, each region’s composite score of the light pollution risk indicator is calculated (see Figure 4).

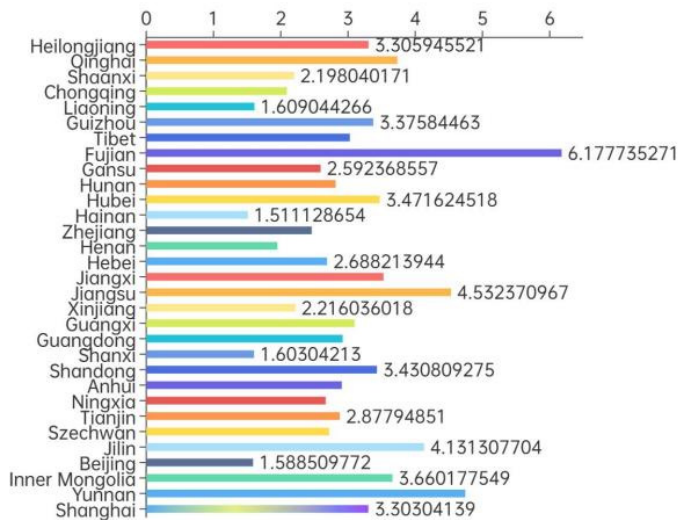


Figure 4. Results of light pollution risk indicators in various regions

Finally, a cluster analysis is used to grade the light pollution risk indicator and get a metric system for the light pollution risk level.

4.2.5 Clustering Analysis of Light Pollution Risk Level

This research calculates a specific area's light pollution risk level through the above calculation method. However, the figure represents the light pollution risk level that must be clarified. Therefore, cluster analysis needs to be used to grade the light pollution risk level and get an explicit standard of light pollution risk levels.

Specifically, this paper aims to cluster the light pollution risk level for each central region in China. By doing the above process, possible standards of light pollution risk levels should also be covered. A hierarchical cluster is used to process the generated data. The process of this project is as follows: in the first place, each sample is regarded as a class, and then the nearest sample (i.e., the group with the smallest distance) is clustered into subclasses. Then, the subclasses of the aggregation are merged according to their inter-class distance.

All the subclasses are aggregated into one large class to compare the effects of different measurement methods and types and select the number of clusters. Finally, it is found that clustering works best when ward connectivity is used to measure differences and to divide regions into five clusters. The clustering results (see Figures 5 and 6) illustrate that these regions can be divided into five categories, namely:

- a. *extremely high risk* The cluster's center point region is close to 6.4172.
- b. *relatively high risk* The cluster's center point region is close to 5.3727.
- c. *general risk* The cluster's center point region is close to 3.9294.
- d. *relatively low risk* The cluster's center point region is close to 3.1175.
- e. *extremely low risk* The cluster's center point region is close to 2.4575.

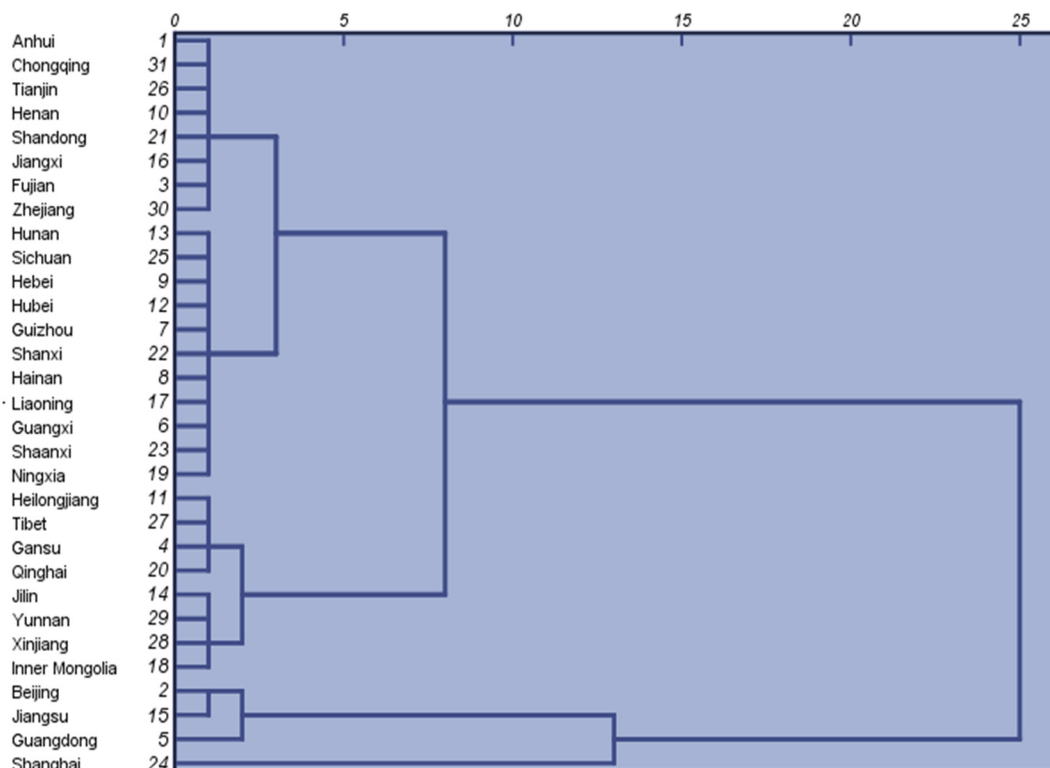


Figure 5. Process of clustering

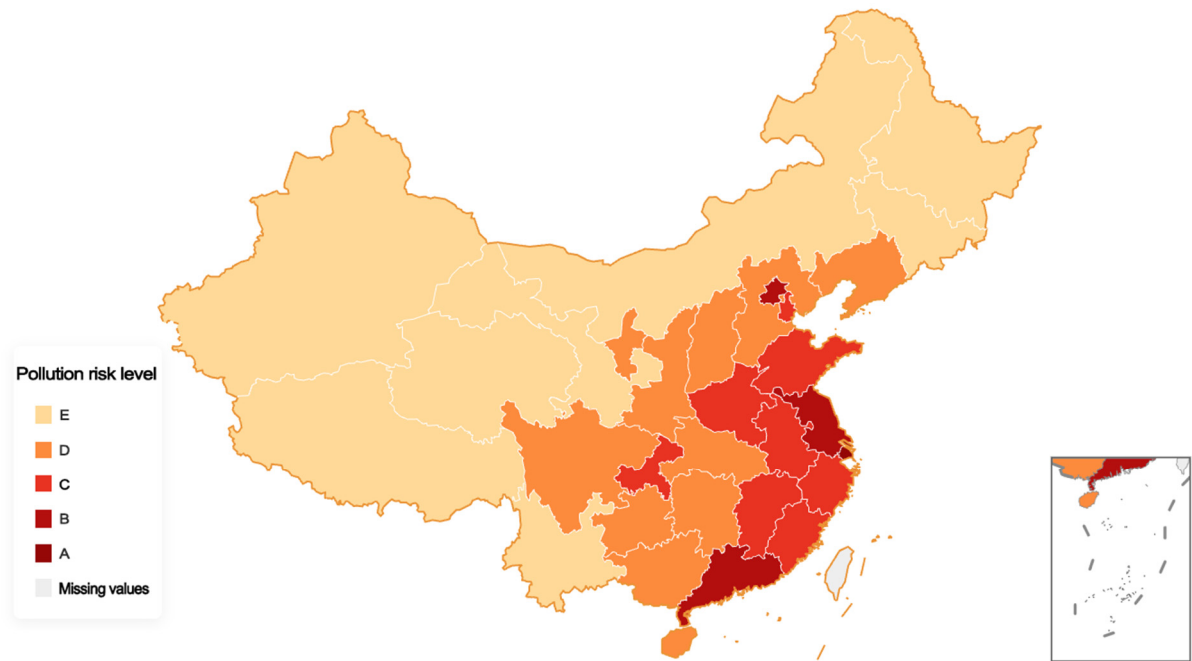


Figure 6. Results of clustering

4.3 Four Diverse Types of Locations

This part mainly explores the application of the metrics system on the four types of locations and the interpretation of their consequences.

The IES model can calculate a specific region’s light pollution risk level based on three types of data: light output indicators, environmental indicators, and social indicators. This result indicates significant differences in light pollution risk levels at different locations. The areas covered by artificial light can be divided into four areas. After comparing and contrasting various data and substantial calculations, the respective values of indicators are determined in the four areas, as shown in Table 4.

Table 4. The respective values of the determined indicators of the four areas

Regional Types	Climate	Population Density	Biodiversity	Illumination Density Distribution	Illumination Level	Average Duration of Light
protected land	++++	+	++++	+	+	+
rural community	+++	++	+++	+	+	++
suburban community	++	++	+	++	+++	+++
urban community	+	++++	+	++++	+++	++++

Significant differences exist in the secondary indicators for different types of areas, which will directly affect the final light pollution risk indicator and its level classification. The IES model can be used to explain these four regions more thoroughly.

Protected land is an area that may refer to a reserve protected from development by a government or private entity because of its ecological, cultural, and natural importance. These areas tend to have relatively abundant biodiversity, leading to increased light pollution risk levels. However, due to the low population density and relatively low light output indicator, the IES model can be applied to calculate grade-specific locations.

A rural community is located in one country or region's most sparsely populated areas and is not easily accessible from urban communities. This area is far from the main commercial and industrial areas and has low population density, illumination density distribution, and illumination level. Nevertheless, compared with urban communities, where the climate and biodiversity are relatively high, it is also necessary to use the IES model to calculate grade-specific sites due to the possibility of numerous agricultural activities in this area.

A suburban community is located in an area of moderate population density in a country and region or is easily accessible from an urban community. These areas usually have fewer commercial areas but mainly residential areas, with relatively low population density and illumination levels. After applying the IES model to assess light pollution risk levels in these areas, the level is slightly lower compared with the urban community.

An urban community is located in a country or region's most densely populated area. These areas have low levels of biodiversity and climate because they have a high population, industrial and commercial activity, non-agricultural population, and little agricultural land. Nonetheless, its illumination output indicators and population density are higher. Thus, the light pollution risk level is generally higher than in other areas.

5. Discussion

This section identifies three possible strategies to cope with light pollution. As shown in 4.2.4, several effects of light pollution are elaborated on, which serve as the foundation for this section. Section 5.1 discusses the potential impacts of specific actions to carry out those strategies on these effects of light pollution, whereas section 5.2 centers on which strategy plays the most influential role in the two selected locations and the specific mechanism of how the very strategy affects light pollution risk levels for the locations.

5.1 Effects of Intervention Strategies

Based on the IES Model, various intervention strategies emerge, mainly restricting luminaires' power, normalizing service time, and bolstering vegetation coverage. While in the IES Model, the main factors affecting the light pollution risk level in a specific area are light output, environmental factors, and social factors, the last categories are mainly targeted at the objective level, which can hardly be changed through human intervention.

The first issue is the significant effects of light pollution on humans and other creatures. On the one hand, light pollution causes light loss, aesthetic ruin, regular life disruption, and safety issues (Cinzano, 2002). These four angles are strongly related to population density. Therefore, the above social indicators have involved the influence of indicators on humans. On the other hand, light pollution also affects other animals, which consequently causes environmental degradation, ecological imbalance, and the loss of magnificent night skies. Environmental indicators include environmental pollution, energy waste, and threats to ecological balance. At the same time, the loss of the priceless night sky is difficult to quantify, so the model incorporates the influence on other creatures in the above discussion. A preliminary outlook of these effects is presented in Figure 7.

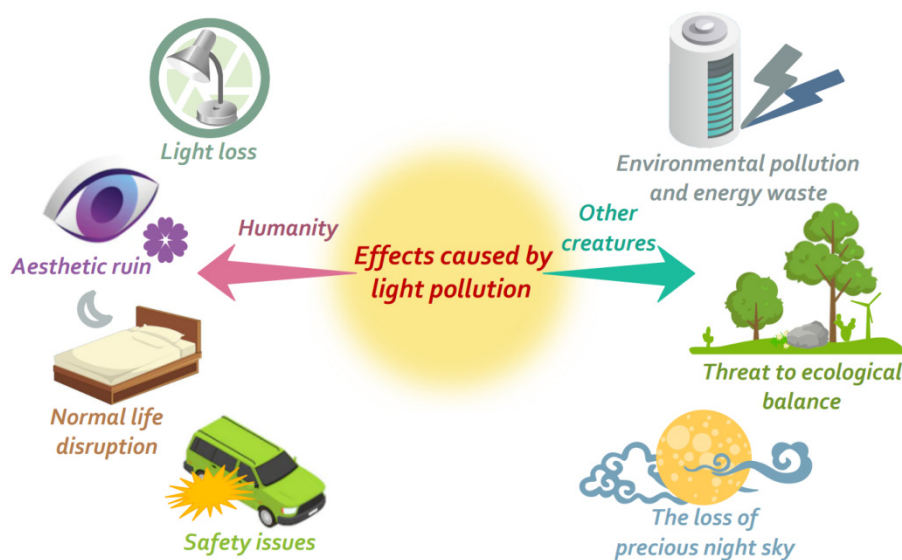


Figure 7. Effects caused by light pollution

5.1.1 Restricting Luminaires' Power

The restricted luminaires' power is closely related to the evaluation indicator of illumination level in the IES Model. This strategy of limiting the power of lamps can be defined in terms of energy, reducing the luminance loss, and improving the safety factor by influencing the physical characteristics of the lamps.

For instance, specific intervention strategies can be implemented using low-power *light-emitting diode* (LED) lighting. LED lighting equipment has many advantages; it has a small volume and power, has an apparent energy-saving effect, and does not have ultraviolet light. It will not cause *ultraviolet* (UV) damage to buildings and the night sky, especially at night. LED lighting can make all the light emitted by the luminaires spread on the target object, and LED lighting is easy to hide, soft light without glare, with no light pollution to residents and the environment. Therefore, the light pollution risk level in a specific area can be effectively reduced through intervention strategies to influence the illuminance level of the area.

Nevertheless, the power of the luminaries is reduced with inadequate consideration. In that case, it may lead to problems such as insufficient brightness, indirectly producing potential impacts like raising traffic accident rates and rising crime rates. Therefore, to achieve the necessary illumination, it is necessary to build optical sources for function and landscape illumination. The luminaires' layout should be matched for low-brightness light sources instead of a few high-brightness ones.

5.1.2 Normalizing Service Time

The normalization of service time echoes the evaluation indicator of the average duration of light in the IES Model. The strategy of normalizing service time can be defined from the user's point of view to influence the light pollution risk level by limiting the user's behavior.

For example, this intervention strategy can limit the dynamic, colored lighting time in and around residential areas. This strategy can also replace some luminaires in or around residential areas with voice-controlled lights to reduce the ineffective lighting time at night, the average light duration, and thus the light pollution risk level. In addition, it is possible to improve relevant legal regulations, such as setting dynamic curfew hours according to the different lengths of day and night in different seasons and turning off any non-essential lighting facilities after curfew hours. These interventions aim at the average duration of light and have potential implications for other aspects of society. Nevertheless, this intervention strategy also has some adverse effects. Replacing voice-controlled lamps may increase the noise pollution risk level, and the unified closing time of luminaires may inconvenience residents. Moreover, reducing the average duration of light in areas with low pedestrian flow may indirectly increase the social crime rate.

5.1.3 Bolstering the Vegetation Coverage

In the IES Model, the improvement of vegetation coverage is closely related to various environmental indicators, such as biodiversity and air quality. The improvement of vegetation coverage is based on the light exposure environment. Through a reasonable layout of planting, a light-absorbing environment is provided around artificial light equipment to reduce various kinds of light pollution generated in lighting and thus reduce the light pollution risk level. In addition, improving a green area can also promote air quality, and increasing also regulates the light pollution risk level. Therefore, increasing vegetation coverage can play a role in maintaining the balance of the ecological environment, and environmental pollution and energy waste can be effectively managed as well.

For example, the government or authorities can influence specific intervention strategies, and the construction of vegetation coverage can be invested. Meanwhile, vegetation and lamps can be combined with planning to create a green environment for the region to effectively reduce the light pollution risk level. However, this strategy may have the potential impact of excessive management pressure on the landscape service industry.

5.2 Optimization for the Intervention Strategies

The above points to possible, more practical intervention strategies by community officials or local groups to reduce the light pollution risk level in a particular area. Next, this section evaluates the effectiveness of this intervention strategy. Three specific intervention strategies are first summarized, and protected land and urban communities are selected to evaluate their effectiveness.

Three specific intervention strategies are as follows. *Strategy I*: Using multiple low-brightness light sources to replace a few high-brightness light sources. *Strategy II*: Limiting dynamic, colored lighting in or around residential areas to be turned off after a certain time at night. *Strategy III*: Increasing the area covered by regional vegetation. In general, the calculation process is visualized in Figure 8.

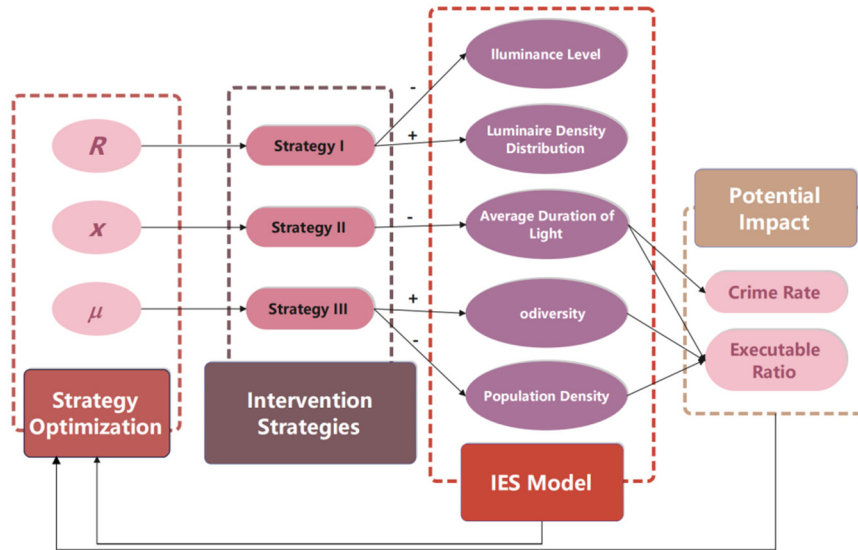


Figure 8. Non-linear programming of the model

5.2.1 Strategy I: Replacing of High-Brightness Luminaires

Specific measures are as follows. Community officials or local groups stipulate that the area should use multiple low-brightness light sources instead of a few high-brightness light sources, thus reducing the secondary indicator illuminance level in the IES model. However, luminaire density distribution, a secondary indicator in the IES model, is also increased. For this reason, the calculation is as follows.

After dimensional analysis and calculation, it is stipulated that:

$$I_i L_i S_i = Const$$

In the formula, the illuminance level of region i is the luminaire density distribution of region i and is the regional area of region i . $Const$ represents a definite constant called the optical output synthesis constant. The regional area S is a particular indicator for a specific area, so the illuminance level and luminaire density distribution are inversely proportional.

After that, the substitution indicator is specified as R , which represents the ratio of the replacement number of multiple low-brightness light sources replacing a few high-brightness light sources in the region to the total number of light sources in the region:

$$R = \frac{Q}{SL}$$

In the formula, Q is the replacement quantity, S is the regional area, and L is the luminaire density distribution of the region.

Finally, for calculating non-linear programming, part of the calculation in the IES model is selected instead of calculating the final light pollution risk indicator. The corresponding weight obtained by EWM is used in the IES model. Weighted summation of illuminance level and luminaire density distribution is conducted:

$$Result_i = \omega_I I_i + \omega_L L_i$$

In the formula, $Result_i$ is the result indicator obtained by combining illuminance level and luminaire density distribution in region i . Moreover, ω_I and ω_L are the corresponding weights of illuminance level, and EWM calculates luminaire density distribution.

Next, non-linear programming is used to analyze protected land and the urban community to determine the optimal alternative indicator R for the two areas.

a) Protected land

The impact of *Strategy I* on protected land is discussed in detail in 5.1.1. It is argued that protected land and different types of areas have significant differences in the regional area, illuminance level, and luminaire density distribution (see Table 4). Therefore, the average value of these three indicators for each protected land is

considered the key to obtaining the world average optical output synthesis constant for protected land. The calculation formula is as follows:

$$\overline{Const} = \frac{\sum_{i=1}^n I_i L_i S_i}{n}$$

$$\bar{S} = \frac{\sum_{i=1}^n S_i}{n}, \quad \bar{L} = \frac{\sum_{i=1}^n L_i}{n}, \quad \bar{I} = \frac{\sum_{i=1}^n I_i}{n}$$

Among them, n is the total number of samples of protected land. As mentioned above, I_i is the illuminance level of region i , and \bar{I} is its mean value. L_i is the luminaire density distribution of region i , and \bar{L} is its mean value. S_i is the regional area of region i , \bar{S} is the average regional area.

Additionally, \overline{Const} is the calculated global average optical output synthesis constant, which is taken as the optical output synthesis constant for protected land; \bar{S} , the average regional area, is taken as the regional area of protected land in the following calculation; \bar{L} and \bar{I} are taken as the original indicators data respectively before the implementation of the strategy.

In addition, since the IES model includes Z-score standardized processing of illuminance level and luminaire density distribution, the results obtained in this part are unitless values due to the dimensional unification not being carried out.

After that, non-linear programming is used to calculate R . The calculation process is as follows:

$$\begin{aligned} \min \quad & Result_i = \omega_I I_i + \omega_L L_i \\ \text{s.t.} \quad & I_i L_i \bar{S} = \overline{Const} \\ & 0 \leq R = \frac{Q}{\bar{S} L_i} \leq 1 \\ & L_i = \bar{L} + R \bar{I} \geq 0 \\ & I_i = \bar{I} - R \bar{I} \geq 0 \end{aligned}$$

Finally, after non-linear programming, when the minimum value is obtained, $R=27.721\%$. This indicates that for *Strategy I* in protected land, the light pollution risk level is minimized when low-brightness light sources replace 27.7% of high-brightness light sources. R is relatively tiny for protected land and other regions with low illuminance levels and luminaire density distribution, indicating that the calculated results are consistent with the actual situation.

b) Urban community

Similarly, the impact of *Strategy I* on the urban community is discussed in detail in 5.1.1. In the same way as the above method to obtain the optimal alternative indicator R for protected land, non-linear programming operations are also conducted for the urban community. The calculation process is not repeated here.

Finally, this research calculates $R=49.724\%$ when the minimum value is obtained. This indicates that when low-brightness light sources replace 49.7% of high-brightness light sources, the light pollution risk level becomes minimal for the urban community. R is relatively large for urban communities and other areas with high illuminance levels and luminaire density distribution, indicating that the calculated results are consistent with the actual situation.

5.2.2 Strategy II: Restricting Service Time of Luminaires

The dynamic and colored lighting in or around residential areas should be restricted to be turned off after a particular time at night to reduce the average duration of light in the IES model. However, as this strategy inconveniences residents, it may also increase the crime rate. So, the calculation is as follows.

First, the mean of the calculated average duration of light in the region is used as the indicator before the implementation of the strategy:

$$\bar{D} = \frac{\sum_{i=1}^n D_i}{n}$$

Among them, n is the average duration of light in the region where the total number of samples is i , and \bar{D} is its mean.

Then, it is stipulated that the lighting is turned off for x hours at night, whereas D' is the indicator of the average

duration of light after the implementation of the strategy:

$$D' = \frac{12 - x}{8} \bar{D}$$

It is significant to specify μ_i as the executable ratio of this strategy to the region i . The relationship between this ratio and x must be determined by investigating relevant literature and data for specific regions.

Finally, a part of the calculation in the IES model is chosen without calculating the final light pollution risk indicator for non-linear programming. The corresponding weight obtained by EWM in the IES model is used to weigh the indicator of the average duration of light.

$$Result_i = \mu_i \omega_D D'_i$$

a) Protected land

After searching relevant information for protected land, the relationship between executable ratio μ_i and x is as follows:

$$\mu_i = 0.8 \frac{1}{12 - x}$$

Therefore, based on non-linear programming, the calculation process is as follows:

$$\begin{aligned} \min \quad & Result_i = \mu_i \omega_{Di} D'_i \\ \text{s. t.} \quad & D' = \frac{12 - x}{8} \bar{D} \\ & 0 \leq x < 12 \\ & \mu_i = 0.8 \frac{1}{12 - x} \leq 1 \end{aligned}$$

Finally, it is concluded that $x=4.672$ when the minimal $Result_i$ are obtained. This suggests that *Strategy II* is optimal for protected land: limiting movement in or around residential areas and color lighting to be turned off around 7 p.m.

b) Urban community

After a search for relevant information about the urban community, the relationship between the executable ratio and x is as follows:

$$\mu_i = 0.3 \frac{1}{12 - x}$$

Similarly, with the non-linear programming method above, it is concluded that $x=1.529$ when $Result_i$ is the minimal value for an urban community. This suggests that *Strategy II* is optimized for urban communities: limiting the dynamic, colored lighting inside or around residential areas to be turned off at around 10 p.m.

5.2.3 Strategy III: Increasing the Vegetation Coverage

Specific measures are to increase the vegetation cover area of the region so that the vegetation cover ratio is μ , thereby reducing the secondary indicator, namely the biodiversity indicator in the IES model, which has been positively processed. However, based on the feasibility of increasing vegetation coverage, the increase in regional population density should decrease accordingly, so the calculation is as follows.

First, the mean of biodiversity in the area is calculated, which is an indicator before implementing the strategy:

$$\bar{B} = \frac{\sum_{i=1}^n B_i}{n}$$

Among them, B_i is the biodiversity indicator of region i , whereas \bar{B} is its average value.

Moreover, the following process is used to calculate part of the calculation instead of calculating the final indicator by the IES model to facilitate the non-linear programming operation. The indicator of biodiversity after implementing the strategy is calculated as follows:

$$B' = \sigma \mu \omega_{Bi} \bar{B}$$

Among them, B' is the indicator after implementing the biodiversity strategy, and ω_{Bi} is the weight calculated

by EWM in the IES model. Importantly, the relationship between executable ratio σ and population density for a given area is defined as follows:

$$\sigma = \frac{1}{\omega_p \bar{P}}$$

$$\bar{P} = \frac{\sum_{i=1}^n P_i}{n}$$

In the formula, n is the total number of samples, and ω_p is the corresponding weight of population density calculated by EWM in the IES model; P_i is the indicator data of population density, and \bar{P} is its mean value.

Finally, the results are weighed, and the following relationship is attained:

$$Result_i = \omega_B B'_i$$

Among them, $Result_i$ is the corresponding weight of biodiversity calculated by EWM in the IES model.

a) Protected land

Based on non-linear programming, the calculation process is as follows:

$$\begin{aligned} \min \quad & Result_i = \omega_B B'_i \\ \text{s.t.} \quad & B' = \sigma \mu \omega_{B_i} \bar{B} \\ & 0 \leq \mu \leq 1 \end{aligned}$$

Finally, when the minimal $Result_i$ is obtained, $\mu=0.652$, which indicates that the optimization of *Strategy III* for protected land is to increase the area covered by regional vegetation so that the vegetation coverage ratio is about 65%.

b) Urban community

Similarly, using the non-linear programming method, it can be concluded that for the urban community, when $Result_i$ reaches its minimum, $\mu=0.339$. This result shows that the optimization of *Strategy III* for the urban community is to increase the area covered by regional vegetation so that the vegetation coverage ratio is about 34%.

6. Sensitivity Analysis

A sensitivity analysis is finally conducted on all secondary indicators mentioned in the IES model (see Figure 9).

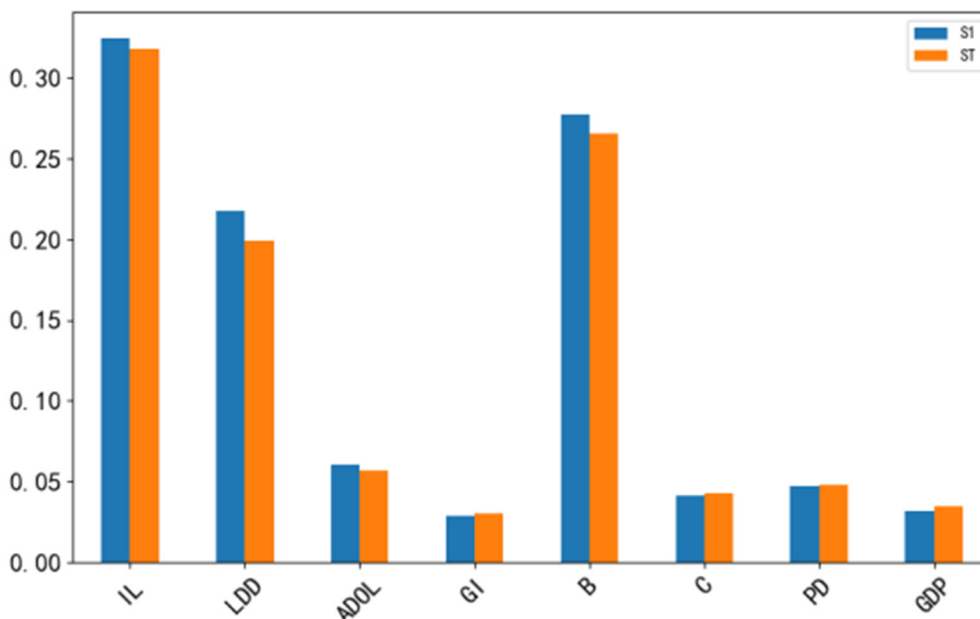


Figure 9. Sensitivity analysis

The influence degree of these secondary indicators on the results of light pollution risk levels is considered when

specific changes occur, that is, their contribution to the variance of light pollution risk levels. The results show sensitivities of all secondary indicators in the IES model and are within the reasonable range, indicating the rationality and comprehensiveness of the model.

7. Concluding Remarks

This paper proposes a mathematical model for determining and evaluating the light pollution risk level in a region. Two weighting methods, AHP and EWM, are used to perform a joint analysis of subjective experience and objective data on the evaluation ladder of the light pollution risk level to restore the model's credibility. The model's viability is increased by utilizing multilevel indicators that accurately represent the light pollution risk level. Among them, with luminous remote sensing and *the National Statistical Yearbook* as the source, the data of secondary indicators are quantified and gathered by *K*-means clustering and other techniques. Also, to ensure the model's accuracy, *Z*-score standardization and other pretreatment techniques are used to increase the model's convergence rate and make the features of various dimensions numerically measurable and calculable.

The present study contributes to evaluating light pollution risk levels in specific areas. For one thing, it considers multiple factors and enriches mathematical methods for evaluating light pollution risk levels. For another, the IES model can help agencies develop intervention strategies towards light pollution, thereby reducing its impact. As for existing limitations, this study focuses on most factors that can be used to evaluate light pollution, but some specific individual factors, such as surface albedo and human eye sensitivity, still need to be addressed. Therefore, future research is expected to investigate their impact by comprehensively and systematically evaluating the light pollution risk level and explore how the IES model can be further implemented.

Acknowledgments

We acknowledge financial and technical support from *Brightopia*, where we work part-time as teaching and research assistants. Sincere gratitude also goes to Jialiang Chen for his insightful guidance and constructive feedback on content relevance, content sufficiency, organization, and language quality in several versions of this paper. All remaining infelicities are attributed to the authors.

References

- Alamús, R., Bará, S., Corbera, J., Escofet, J., Palà, V., Pipia, L., & Tardà, A. (2017). Ground-based hyperspectral analysis of the urban nightscape. *ISPRS Journal of Photogrammetry and Remote Sensing*, *124*, 16–26. <https://doi.org/10.1016/j.isprsjprs.2016.12.004>
- Bertolo, A., Binotto, R., Ortolani, S., & Sapienza, S. (2019). Measurements of night sky brightness in the veneto region of italy: Sky quality meter network results and differential photometry by digital single lens reflex. *Journal of Imaging*, *5*(5), 56. <https://doi.org/10.3390/jimaging5050056>
- Bouroussis, C. A., & Topalis, F. V. (2020). Assessment of outdoor lighting installations and their impact on light pollution using unmanned aircraft systems-The concept of the drone-gonio-photometer. *Journal of Quantitative Spectroscopy and Radiative Transfer*, *253*, 107155. <https://doi.org/10.1016/j.jqsrt.2020.107155>
- Brayley, O., How, M., & Wakefield, A. (2022). The biological effects of light pollution on terrestrial and marine organisms. *International Journal of Sustainable Lighting*, *24*(1), 13–38.
- Cavazzani, S., Ortolani, S., Bertolo, A., Binotto, R., Fiorentin, P., Carraro, G., ... & Zitelli, V. (2020). Sky Quality Meter and satellite correlation for night cloud-cover analysis at astronomical sites. *Monthly Notices of the Royal Astronomical Society*, *493*(2), 2463–2471. <https://doi.org/10.1093/mnras/staa416>
- Chen, F., & Peng, S. (2013). City night light pollution impact on trees. *Journal of Ecological Environment*, *22*(7), 1193–1198. <https://doi.org/10.16258/j.cnki.1674-5906.2013.07.009>
- Cinzano, P. (2002). *IDA European Meeting Report*. Italy: Light Pollution Science and Technology Institute.
- Czyżewski, D. (2023). The photometric test distance in luminance measurement of light-emitting diodes in road lighting. *Energies*, *16*(3), 1199. <https://doi.org/10.3390/en16031199>
- de Miguel, A. S., Zamorano, J., Castaño, J. G., & Pascual, S. (2014). Evolution of the energy consumed by street lighting in Spain estimated with DMSP-OLS data. *Journal of Quantitative Spectroscopy and Radiative Transfer*, *139*, 109–117. <https://doi.org/10.1016/j.jqsrt.2013.11.017>
- Ding, K., Zhang, H., & Li, N. (2014). Urban light pollution presents a situation investigation and evaluation method of the case study. *Journal of Environmental Pollution and Control*, *4*(5), 111. <https://doi.org/10.15985/j.cnki.1001-3865.2014.05.026>
- Dong, X. (2008). Discussion on the control of urban environmental pollution by landscaping. *Northern*

- Horticulture*, (09), 141–142.
- Elvidge, C. D., Baugh, K. E., Dietz, J. B., Bland, T., Sutton, P. C., & Kroehl, H. W. (1999). Radiance calibration of DMSP-OLS low-light imaging data of human settlements. *Remote Sensing of Environment*, 68(1), 77–88. [https://doi.org/10.1016/S0034-4257\(98\)00098-4](https://doi.org/10.1016/S0034-4257(98)00098-4)
- Falchi, F., Cinzano, P., Duriscoe, D., Kyba, C. C., Elvidge, C. D., Baugh, K., Portnov, B. A., Rybnikova, N. A., & Furgoni, R. (2016). The new world atlas of artificial night sky brightness. *Science Advances*, 2(6), e1600377. <https://doi.org/10.1126/sciadv.1600377>
- Falchi, F., Cinzano, P., Elvidge, C. D., Keith, D. M., & Haim, A. (2011). Limiting the impact of light pollution on human health, environment and stellar visibility. *Journal of Environmental Management*, 92(10), 2714–2722. <https://doi.org/10.1016/j.jenvman.2011.06.029>
- Frontczak, M., & Wargocki, P. (2011). Literature survey on how different factors influence human comfort in indoor environments. *Building and Environment*, 46(4), 922–937. <https://doi.org/10.1016/j.buildenv.2010.10.021>
- Fryc, I., Bara, S., Aubé, M., Barentine, J. C., & Zamorano, J. (2022). On the relation between the astronomical and visual photometric systems in specifying the brightness of the night sky for mesopically adapted observers. *Leukos*, 18(4), 447–458. <https://doi.org/10.1080/15502724.2021.1921593>
- Galatanu, C. D., Husch, M., Canale, L., & Lucache, D. (2019, June). Targeting the light pollution: A study case. In *2019 IEEE International Conference on Environment and Electrical Engineering and 2019 IEEE Industrial and Commercial Power Systems Europe (EEEIC/I&CPS Europe)* (pp. 1–6). IEEE. <https://doi.org/10.1109/EEEIC.2019.8783515>
- Galloway, T., Olsen, R. N., & Mitchell, D. M. (2010). The economics of global light pollution. *Ecological Economics*, (3), 658–665. <https://doi.org/10.1016/j.ecolecon.2009.10.003>
- Gao, Z., Lu, Y., & Chen, Y. (2019). Urban light pollution and its control measures. *Environmental Protection*, 47(13), 44–46. <https://doi.org/10.14026/j.cnki.0253-9705.2019.13.009>
- Gaston, K. J., Bennie, J., Davies, T. W., & Hopkins, J. (2013). The ecological impacts of nighttime light pollution: A mechanistic appraisal. *Biological Reviews*, 88(4), 912–927. <https://doi.org/10.1111/brv.12036>
- Gronkowski, P., Tralle, I., & Wesolowski, M. (2018). Visibility of comets during their outbursts and the night sky light pollution—Use the Bortle scale. *Astronomische Nachrichten*, 339(1), 37–45. <https://doi.org/10.1002/asna.201713387>
- Hänel, A., Posch, T., Ribas, S. J., Aubé, M., Duriscoe, D., Jechow, A., ... Kyba, C. C. (2018). Measuring night sky brightness: Methods and challenges. *Journal of Quantitative Spectroscopy and Radiative Transfer*, 205, 278–290. <https://doi.org/10.1016/j.jqsrt.2017.09.008>
- Hao, Y., Zhang, P., & Gao, F. (2022). Light pollution management policy and LED advertising screen interference light limit standard analysis. *Journal of Environmental Monitoring in China*, 38(03), 199–206. <https://doi.org/10.19316/j.issn.1002-6002.2022.03.22>
- Hara, M., Okada, S., Yagi, H., Moriyama, T., Shigehara, K., & Sugimori, Y. (2010). Progress for stable artificial lights distribution extraction accuracy and estimation of electric power consumption by means of dmsp/ols nighttime imagery. *International Journal of Remote Sensing and Earth Sciences (IJReSES)*, 1(1). <http://dx.doi.org/10.30536/j.ijreses.2004.v1.a1326>
- Hölker, F., Wolter, C., Perkin, E. K., & Tockner, K. (2010). Light pollution as a biodiversity threat. *Trends in Ecology & Evolution*, 25(12), 681–682. <https://doi.org/10.26607/ijsl.v24i1.121>
- Hölker, F., Wurzbacher, C., Weißenborn, C., Monaghan, M. T., Holzhauser, S. I., & Premke, K. (2015). Microbial diversity and community respiration in freshwater sediments influenced by artificial light at night. *Philosophical Transactions of the Royal Society B: Biological Sciences*, 370(1667), 20140130. <https://doi.org/10.1098/rstb.2014.0130>
- Hussein, A. A. A., Bloem, E., Fodor, I., Baz, E. S., Tadros, M. M., Soliman, M. F. M., El-Shenawy, N. S., & Koene, J. M. (2021). Slowly seeing the light: An integrative review on ecological light pollution as a potential threat for mollusks. *Environmental Science and Pollution Research International*, 28(5), 5036–5048. <https://doi.org/10.1007/s11356-020-11824-7>
- Jack, N., Soo, L. H., & Gon, K. (2018). Light pollution: Is there an environmental kuznets curve? *Sustainable Cities and Society*, 42, 337–343.

- Karpińska, D., & Kunz, M. (2022). Device for automatic measurement of light pollution of the night sky. *Scientific Reports*, 12(1), 16476.
- Knop, E., Zoller, L., Ryser, R., Gerpe, C., Hörler, M., & Fontaine, C. (2017). Artificial light at night as a new threat to pollination. *Nature*, 548(7666), 206–209. <https://doi.org/10.1038/nature23288>
- Korner, P., von Maravic, I., & Haupt, H. (2022). Birds and the ‘Post Tower’ in Bonn: A case study of light pollution. *Journal of Ornithology*, 163(3), 827–841.
- Kuffer, M., Pfeffer, K., Sliuzas, R., Taubenböck, H., Baud, I., & van Maarseveen, M. (2018). Capturing the urban divide in nighttime light images from the International Space Station. *Ieee Journal of Selected Topics in Applied Earth Observations and Remote Sensing*, 11(8), 2578–2586. <https://doi.org/10.1109/JSTARS.2018.2828340>
- Kyba, C. C., Kuester, T., Sánchez de Miguel, A., Baugh, K., Jechow, A., Hölker, F., ... Guanter, L. (2017). Artificially lit surface of Earth at night increasing in radiance and extent. *Science Advances*, 3(11), e1701528. <https://doi.org/10.1126/sciadv.1701528>
- Kyba, C. C., Tong, K. P., Bennie, J., Birriel, I., Birriel, J. J., Cool, A., ... Gaston, K. J. (2015). Worldwide variations in artificial skyglow. *Scientific Reports*, 5(1), 8409.
- Levin, N., Kyba, C. C., & Zhang, Q. (2019). Remote sensing of night lights—beyond DMSP. *Remote Sensing*, 11(12), 1472. <https://doi.org/10.3390/rs11121472>
- Lin, J., & Shi, W. (2020). Statistical correlation between monthly electric power consumption and VIIRS nighttime light. *ISPRS International Journal of Geo-Information*, 9(1), 32. <https://doi.org/10.3390/ijgi9010032>
- Longcore, T., & Rich, C. (2004). Ecological light pollution. *Frontiers in Ecology and the Environment*, 2(4), 191–198.
- Luginbuhl, C. B., Walker, C. E., & Wainscoat, R. J. (2009). Lighting and astronomy. *Physics Today*, 62(12), 32–37. <https://doi.org/10.1063/1.3273014>
- Navara, K. J., & Nelson, R. J. (2007). The dark side of light at night: Physiological, epidemiological, and ecological consequences. *Journal of Pineal Research*, 43(3), 215–224. <https://doi.org/10.1111/j.1600-079x.2007.00473.x>
- Nian, Y., Liu, W., & Fan, Z. (2005). Urban environment and light pollution. *Journal of Shaanxi Normal University (Natural Science Edition)*, (S1), 74–75.
- Ouyang, J. Q., de Jong, M., van Grunsven, R. H., Matson, K. D., Haussmann, M. F., Meerlo, P., ... Spoelstra, K. (2017). Restless roosts: Light pollution affects behavior, sleep, and physiology in a free living songbird. *Global Change Biology*, 23(11), 4987–4994. <https://doi.org/10.1111/gcb.13756>
- Pauwels, J., Le Viol, I., Bas, Y., Valet, N., & Kerbiriou, C. (2021). Adapting street lighting to limit light pollution’s impacts on bats. *Global Ecology and Conservation*, 28, e01648. <https://doi.org/10.1016/j.gecco.2021.e01648>
- Pollard, N. (2001). Guide on the limitation of the effects of obtrusive light from outdoor lighting installations. *Symposium - International Astronomical Union*, 196, 77–80.
- Prakash, R., Hossain, A. M., Pal, U. N., Kumar, N., Khairnar, K., & Mohan, M. K. (2017). Dielectric barrier discharge based mercury-free plasma UV-lamp for efficient water disinfection. *Scientific Reports*, 7(1), 17426.
- Puschnig, J., Wallner, S., Posch, T., & Binder, F. (2019). Quantifying circalunar periodicity, long-term trends and seasonal variations in the night sky brightness based on the Austrian SQM network. *Light Pollution: Theory*, 1. <https://doi.org/10.5281/zenodo.3654028>
- Ścieżor, T. (2020). The impact of clouds on the brightness of the night sky. *Journal of Quantitative Spectroscopy and Radiative Transfer*, 247, 106962. <https://doi.org/10.1016/j.jqsrt.2020.106962>
- Ścieżor, T. (2021). Effect of street lighting on the urban and rural night-time radiance and the brightness of the night sky. *Remote sensing*, 13(9), 1654.
- Shi, K., Yu, B., Huang, Y., Hu, Y., Yin, B., Chen, Z., ... Wu, J. (2014). Evaluating the ability of NPP-VIIRS nighttime light data to estimate the gross domestic product and the electric power consumption of China at multiple scales: A comparison with DMSP-OLS data. *Remote Sensing*, 6(2), 1705–1724. <https://doi.org/10.3390/rs6021705>
- Shing, C., Pun, J., & So, C. W. (2012). Night-sky brightness monitoring in Hong Kong. *Environmental Monitoring and Assessment*, 184(4), 2537.

- Simons, A. L., Yin, X., & Longcore, T. (2020). High correlation but high scale-dependent variance between satellite measured night lights and terrestrial exposure. *Environmental Research Communications*, 2(2), 021006. <https://doi.org/10.1088/2515-7620/ab7501>
- Słomiński, S., & Krupiński, R. (2018). Luminance distribution projection method for reducing glare and solving object-floodlighting certification problems. *Building and Environment*, 134, 87–101. <https://doi.org/10.1016/j.buildenv.2018.01.019>
- Su, X. (2011). *Comprehensive Evaluation of Residential Light Pollution* (Ph.D. Dissertation, Tianjin University).
- Tabaka, P. (2020). Pilot measurement of illuminance in the context of light pollution performed with an unmanned aerial vehicle. *Remote Sensing*, 12(13), 2124. <https://doi.org/10.3390/rs12132124>
- Van Doren, B. M., Horton, K. G., Dokter, A. M., Klinck, H., Elbin, S. B., & Farnsworth, A. (2017). High-intensity urban light installation dramatically alters nocturnal bird migration. *Proceedings of the National Academy of Sciences*, 114(42), 11175–11180. <https://doi.org/10.1073/pnas.1708574114>
- Vandersteen, J., Kark, S., Sorrell, K., & Levin, N. (2020). Quantifying the impact of light pollution on sea turtle nesting using ground-based imagery. *Remote Sensing*, 12(11), 1785. <https://doi.org/10.3390/rs12111785>
- Wakefield, A., Broyles, M., Stone, E. L., Harris, S., & Jones, G. (2018). Quantifying the attractiveness of broad spectrum street lights to aerial nocturnal insects. *Journal of Applied Ecology*, 55(2), 714–722. <https://doi.org/10.1111/1365-2664.13004>
- Zamorano, J., de Miguel, A. S., Ocaña, F., Pila-Diez, B., Castaño, J. G., Pascual, S., ... & Nieves, M. (2016). Testing sky brightness models against radial dependency: A dense two-dimensional survey around the city of Madrid, Spain. *Journal of Quantitative Spectroscopy and Radiative Transfer*, 181, 52–66. <https://doi.org/10.1016/j.jqsrt.2016.02.029>
- Zhang, Q., Yang, C., & Huang, Y. (2007). The concept and method of urban landscape lighting design in mountainous areas along the river. *Journal of Chongqing Jianzhu University*, (04), 27–30+65.
- Zhang, T., Wang, R., Chen, Y., Shen, Y., Yuan, B., & Chen, Y. (2019). Eight kinds of greening tree species for urban lighting physiological adaptability. *Journal of Forest and the Environment*, 39(04), 424–430. <https://doi.org/10.13324/j.cnki.jfcf.2019.04.015>
- Zhao, H., & Xiang, D. (2003). Principles of urban lighting environmental planning (2) – The proposal and countermeasures of general light pollution. *Chinese Journal of Lighting Engineering*, 14(2), 56–62.

Copyrights

Copyright for this article is retained by the author(s), with first publication rights granted to the journal.

This is an open-access article distributed under the terms and conditions of the Creative Commons Attribution license (<http://creativecommons.org/licenses/by/4.0/>).